

# Emergence of resonant mode-locking via delayed feedback in quantum dot semiconductor lasers

B. Tykalewicz,<sup>1,2</sup> D. Goulding,<sup>1,2,\*</sup> S. P. Hegarty,<sup>1,2</sup> G. Huyet,<sup>1,2,3</sup>  
T. Erneux,<sup>4</sup> B. Kelleher,<sup>1,5</sup> and E. A. Viktorov<sup>2,3,4</sup>

<sup>1</sup>Tyndall National Institute, University College Cork, Lee Maltings, Dyke Parade, Cork, Ireland

<sup>2</sup>Centre for Advanced Photonics and Process Analysis, Cork Institute of Technology, Cork, Ireland

<sup>3</sup>National Research University of Information Technologies, Mechanics and Optics, St Petersburg, Russia

<sup>4</sup>Optique Nonlinéaire Théorique, Université Libre de Bruxelles, Campus Plaine, B-1050 Bruxelles, Belgium

<sup>5</sup>Department of Physics, University College Cork, Cork, Ireland

\*[david.goulding@tyndall.ie](mailto:david.goulding@tyndall.ie)

**Abstract:** With conventional semiconductor lasers undergoing external optical feedback, a chaotic output is typically observed even for moderate levels of the feedback strength. In this paper we examine single mode quantum dot lasers under strong optical feedback conditions and show that an entirely new dynamical regime is found consisting of spontaneous mode-locking via a resonance between the relaxation oscillation frequency and the external cavity repetition rate. Experimental observations are supported by detailed numerical simulations of rate equations appropriate for this laser type. The phenomenon constitutes an entirely new mode-locking mechanism in semiconductor lasers.

© 2016 Optical Society of America

**OCIS codes:** (140.3490) Lasers, distributed-feedback; (250.5590) Quantum-well, -wire and -dot devices; (140.4050) Mode-locked lasers.

---

## References and links

1. H. Haus, "Mode-locking of lasers," *IEEE J. Sel. Top. Quantum Electron.* **6**, 1173 (2000).
2. J. Javaloyes, J. Mulet, and S. Balle, "Passive mode locking of lasers by crossed-polarization gain modulation," *Phys. Rev. Lett.* **97**, 163902 (2006).
3. T. Erneux and P. Glorieux, *Laser Dynamics* (Cambridge University Press, UK, 2010).
4. R. W. Tkach and A. R. Chraplyvy, "Regimes of feedback effects in 1.5- $\mu\text{m}$  distributed feedback lasers," *IEEE J. Lightwave Technol.* **4**, 1655 (1986).
5. D. O'Brien, S. P. Hegarty, G. Huyet, and A. V. Uskov, "Sensitivity of quantum-dot semiconductor lasers to optical feedback," *Opt. Lett.* **29**, 1072 (2004).
6. T. Heil, I. Fischer, W. Elsässer, J. Mulet, and C. R. Mirasso, "Chaos synchronization and spontaneous symmetry breaking in symmetrically delay coupled semiconductor lasers," *Phys. Rev. Lett.* **86**, 795 (2001).
7. J. F. M. Avila, H. L. D. de S. Cavalcante, and J. R. Rios Leite, "Experimental Deterministic Coherence Resonance," *Phys. Rev. Lett.* **93**, 144101 (2004).
8. A. Hohl and A. Gavrielides, "Bifurcation Cascade in a Semiconductor Laser Subject to Optical Feedback," *Phys. Rev. Lett.* **82**, 1148 (1999).
9. T. Heil, I. Fischer, W. Elsässer, and A. Gavrielides, "Dynamics of Semiconductor Lasers Subject to Delayed Optical Feedback: The Short Cavity Regime," *Phys. Rev. Lett.* **87**, 243901 (2001).
10. M. C. Soriano, J. García-Ojalvo, C. R. Mirasso, and I. Fischer, "Complex photonics: Dynamics and applications of delay-coupled semiconductor lasers," *Rev. Mod. Phys.* **85**, 421 (2013).

11. T. Heil, I. Fischer, and W. Elsässer, "Coexistence of low-frequency fluctuations and stable emission on a single high-gain mode in semiconductor lasers with external optical feedback," *Phys. Rev. A* **58**, R2672 (1998).
12. S. Azouigui, B. Kelleher, S. P. Hegarty, G. Huyet, B. Dagens, F. Lelarge, A. Accard, D. Make, O. Le Gouezigou, K. Merghem, A. Martinez, Q. Zou, and A. Ramdane, "Coherence collapse and low-frequency fluctuations in quantum-dash based lasers emitting at  $1.57\ \mu\text{m}$ ," *Opt. Express* **15**, 014155 (2007).
13. K. Lüdge, M. J. P. Bormann, E. Malić, P. Hövel, M. Kuntz, D. Bimberg, A. Knorr, and E. Schöll, "Turn-on dynamics and modulation response in semiconductor quantum dot lasers," *Phys. Rev. B* **78**, 035316 (2008).
14. T. Erneux, E. A. Viktorov, B. Kelleher, D. Goulding, S. P. Hegarty, and G. Huyet, "Optically injected quantum-dot lasers," *Opt. Lett.* **35**, 937–939 (2010).
15. S. P. Hegarty, D. Goulding, B. Kelleher, G. Huyet, M. Todaro, A. Salhi, A. Passaseo, and M. De Vittorio, "Phase-locked mutually coupled  $1.3\ \mu\text{m}$  quantum-dot lasers," *Opt. Lett.* **32**, 3245–3247 (2007).
16. T. Heil, I. Fischer, and W. Elsässer, "Stabilization of feedback-induced instabilities in semiconductor lasers," *J. Opt. B: Quantum Semiclass. Opt.* **2**, 413 (2000).
17. R. Lang, and K. Kobayashi, "External optical feedback effects on semiconductor injection laser properties," *IEEE J. Quantum Electron.* **16**, 347 (1980).
18. E. A. Viktorov, P. Mandel, and G. Huyet, "Long-cavity quantum dot laser," *Opt. Lett.* **32**, 1268 (2007).
19. P. Bak, "The devil's staircase," *Phys. Today* **39**, No. 12, 38 (1986).
20. D. Baums, W. Elsässer, and E. O. Göbel, "Farey tree and devils staircase of a modulated external-cavity semiconductor laser," *Phys. Rev. Lett.* **63**, 155 (1989).
21. F. Y. Lin and J. M. Liu, "Harmonic frequency locking in a semiconductor laser with delayed negative optoelectronic feedback," *Appl. Phys. Lett.* **81**, 3128 (2002).
22. T. Erneux, E. A. Viktorov, and P. Mandel, "Time scales and relaxation dynamics in quantum-dot lasers," *Phys. Rev. A* **76**, 023819 (2007).
23. M. Radziunas, A. G. Vladimirov, E. A. Viktorov, G. Fiol, H. Schmeckebier, and D. Bimberg, "Strong pulse asymmetry in quantum-dot mode-locked semiconductor lasers," *Appl. Phys. Lett.* **98**, 031104 (2011).
24. E. A. Viktorov, D. Goulding, S. P. Hegarty, G. Huyet, T. Erneux, and B. Kelleher, "Feedback-generated periodic pulse trains in quantum dot lasers," *Proc. SPIE* **9134**, 91341F (2014).
25. J. Mørk, J. Mark, and B. Tromborg, "Route to chaos and competition between relaxation oscillations for a semiconductor laser with optical feedback," *Phys. Rev. Lett.* **65**, 1999 (1990).
26. K. Petermann, "External optical feedback phenomena in semiconductor lasers," *IEEE J. Sel. Top. Quantum Electron.* **1**, 480 (1995).
27. E. A. Viktorov, T. Habruseva, S. P. Hegarty, G. Huyet, and B. Kelleher, "Coherence and Incoherence in an Optical Comb," *Phys. Rev. Lett.* **112**, 224101 (2014).
28. A. G. Vladimirov and D. Turaev, "Model for passive mode locking in semiconductor lasers," *Phys. Rev. A* **72**, 033808 (2005).
29. C. Otto, K. Lüdge, A. G. Vladimirov, M. Wolfrum, and E. Schöll, "Delay-induced dynamics and jitter reduction of passively mode-locked semiconductor lasers subject to optical feedback," *New J. Phys.* **14**, 113033 (2012).
30. B. Lingnau, K. Lüdge, W. W. Chow, and E. Schöll, "Failure of the  $\alpha$  factor in describing dynamical instabilities and chaos in quantum-dot lasers," *Phys. Rev. E* **86**, 065201 (2012).

---

## 1. Introduction

Mode-locked lasers and their associated frequency combs have been at the centre of many important advances in technology and fundamental science in recent years. Typically, mode-locking is achieved in one (or a combination) of three ways: via active modulation, saturable absorption or the Kerr effect [1]. In active mode locking the laser resonator contains an active element modulating the output. For example, an electro-optic modulator or a Mach-Zehnder optical modulator synchronized with the laser round-trip can generate short pulses. For passive mode-locking, a saturable absorber - a passive but non-linear element - promotes the generation of a pulsed output. The shortest pulse lengths are achieved with Kerr lens mode-locking, itself a type of passive mode-locking, although self-starting mode-locking is not always achieved. Methods to achieve passive mode-locking in the absence of a saturable absorber, including crossed-polarization gain modulation [2] in vertical-external-cavity surface-emitting lasers for example, have also been proposed but not yet demonstrated. This paper uncovers a new mechanism leading to mode-locking in semiconductor lasers. It takes the form of a resonant mode-locking arising via a locking phenomenon between the two most important time scales in a semiconductor laser: the cavity round-trip frequency and the relaxation oscillation frequency

(ROF). The relaxation oscillations (ROs) in semiconductor lasers quantify the light-matter interaction in the device. The ROs are damped oscillations arising from perturbations to stable operation and represent an oscillating energy exchange between the electric field and the charge carriers. Central to our discovery is the use of external optical feedback to excite the ROs, causing them to become undamped. There are in fact multiple resonances in the system, taking the form of locking tongues with rational ratios between the ROF and the external cavity frequency.

External optical feedback in semiconductor lasers causes many undesirable instabilities mainly due to the relatively large time delay of the feedback compared to the laser time scales [3]. For conventional quantum well (QW) based or bulk semiconductor lasers, it is known that even extremely weak feedback levels can lead to chaotic behaviour [4] while for quantum dot (QD) lasers based on InAs material, the stability is improved remarkably [5]. The dynamics of semiconductor lasers undergoing delayed optical feedback has a rich literature: results include chaos synchronization [6], coherence resonance [7], bifurcation cascades [8] and pulse packages [9] amongst many others (see [10] for a comprehensive set of references). Many studies concentrate on the chaotic regime where two distinct behaviours are identified: namely low frequency fluctuations (LFF) and coherence collapse (CC) [3, 11]. Fully developed CC is characterized by a completely irregular time series while LFF is characterized by deep intensity drop-outs followed by gradual returns to the initial intensity. Both CC and LFF have been observed for QW devices and quantum dash lasers [12] in contrast to lasers based on QD material. This is largely a consequence of the enhanced damping of the ROs of QD devices [5, 13]. The same property has also been shown to increase stability under optical injection [14] and mutual coupling [15].

Thus, heretofore, chaotic regimes have dominated feedback studies. Indeed, once instabilities appear, the only possible stable lasing obtained is a single external-cavity high-gain mode operation [16]. In this paper we demonstrate experimentally that with QD lasers undergoing optical feedback, a new stable state can be obtained manifesting as a periodic pulse train. The findings are reproduced extremely well using a detailed model tailored for QD lasers. While the famous Lang-Kobayashi rate equations [17] reproduce the observations for conventional semiconductors very well, they are unsuitable for the QD case. This is mainly because high feedback levels and long external cavities are required for the observations of dynamical instabilities. In [18] a long cavity model was introduced accounting well for the observed features in multimode QD experiments. In this work, we show that this model can be further improved by taking into account two distinct delays corresponding to the short laser chip cavity and the long external cavity. We show that the pulse train results from a spontaneous mode-locking amongst external cavity modes (ECMs) which in turn results from a resonance between the ROF and the external cavity repetition rate. It constitutes an entirely new mode-locking mechanism arising through inherent device dynamics.

As mentioned, the locking mechanism arises via rational ratios of the ROF and the external cavity repetition rate. This is reminiscent of mode-locking via the devil's staircase [19–21] and we may speak of a winding number in this context as the ratio of the two frequencies. For a fixed cavity length the ROF can be varied by changing the bias current driving the laser. As the ratio of the ROF and the external cavity frequency varies different winding numbers are obtained and confirmed via time series and radio frequency (RF) measurements. Changing the external cavity round-trip length is shown to produce a similar change in the winding number for a fixed ROF. Numerical simulations show remarkable agreement with the experiment. The system is shown to be highly multistable with certain winding numbers having a larger basin of attraction than others similar to the way in which the simplest fractions have the largest step lengths in the devil's staircase. Because of the varying basin of attraction sizes some traces are far more likely to be observed experimentally.

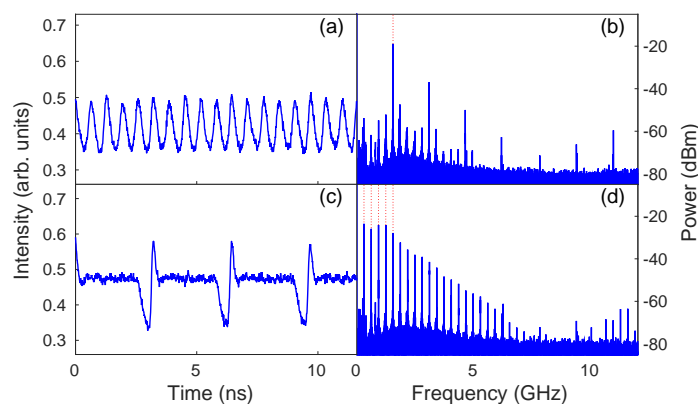


Fig. 1. Experimental time traces showing (a) the nearly sinusoidal oscillation and (c) the fundamental TEP pulse train. The corresponding RF spectra are shown in (b) and (d), respectively. The bias current was 79 mA and the feedback strengths were -16 dB and -15.8 dB respectively. The two frequencies are in a ratio of 1:5 in this case.

## 2. Experimental details

The device used for the experiment is a single mode distributed feedback (DFB) laser. The DFB laser used has an active region consisting of a stack of ten InAs QD layers with a cavity length of 900  $\mu\text{m}$ , as-cleaved facets and a threshold current of 67 mA. The side mode suppression ratio is in excess of 40 dB at all the currents used in the experiments presented here. The external cavity lengths used were quite long, on the order of 0.5 m to 1 m. As is typical with these devices, the RO damping rate is very high as discussed in [13, 14, 22]; so high in fact that the RF spectrum of the free-running device does not display any observable peak in marked contrast to conventional semiconductor lasers. We investigate the behaviour at a fixed external cavity round-trip length of 0.9 m and varying bias currents. For low feedback levels the intensity was constant (modulo noise). Using a variable optical attenuator in the external cavity, the feedback level was increased until continuous operation was lost. In its place a regular, nearly-sinusoidal oscillation was obtained. An example of this oscillatory behaviour for a bias current of 79 mA is shown in Fig. 1(a). The frequency of the oscillation at this bias current was  $\sim 1.55$  GHz, see Fig. 1(b). As the level of feedback is slowly increased the generation of sidebands in the RF spectra, spaced at the round-trip frequency of  $\sim 0.31$  GHz, was observed. Further increase of the feedback strength led to the creation of an extremely distinct pulse train. The train consisted of short pulses followed by broad trailing edge plateaux (TEP) reminiscent of pulses obtained using two section passively mode-locked QD devices in [23] with the frequency of the train matching the round-trip frequency of the external cavity [24]. Figure 1(c) shows an example of this fundamental pulse train. It is quite striking that the pulse train repetition rate, at this bias current, is in a 1:5 resonance with the initial periodic trace, as is clear from the corresponding RF spectra in Figs. 1(b) and 1(d).

As the feedback strength is further increased, the output intensity evolves from single to multiple pulses per round-trip. This progression, with increasing feedback strength, continues until a nearly-sinusoidal oscillation at the frequency of the original instability ( $\sim 1.55$  GHz) was obtained. Further increase in the feedback strength resulted in the observation of chaotic intensity output from the laser. The system also displayed noise induced switching between pulse trains and short time itinerancy of single mode operation, indicating that multistability

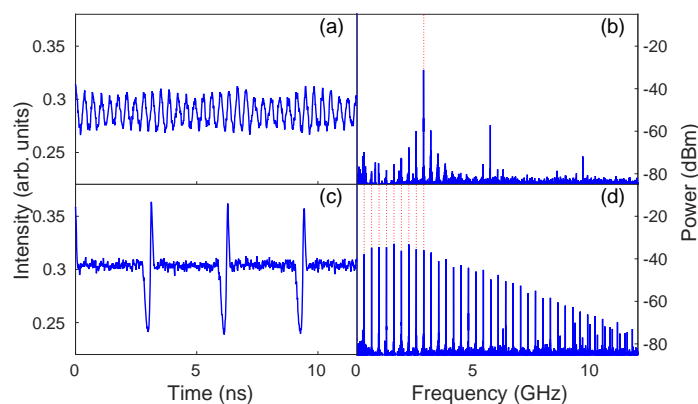


Fig. 2. Experimental time traces showing (a) the nearly sinusoidal oscillation and (c) the fundamental TEP pulse train. The corresponding RF spectra are shown in (b) and (d), respectively. The injection current was 100 mA and the feedback strengths were -12 dB and -6.8 dB. The two frequencies are in a ratio of 1:9 in this case.

is a feature of the system. We note pockets of incoherence, which we define as an absence of rational resonance in the system, are also common and display quasiperiodic intensity traces strongly affected by the inherent noise in the system.

Increasing the bias current leads to similar evolutions. However, the details change: the frequency of the nearly-sinusoidal periodic oscillation increased and again a fundamental pulse train is observed - the TEP pulse train - with a change in the ratio between the two frequencies. The RF trace of the TEP pulses displays many more harmonics than the trace in Fig. 1(d) and the pulses are correspondingly sharper. We continue to increase the current and obtain similar evolutions in each case. The case for a 1:9 resonance is shown in Fig. 2. We find resonances up to and including 1:11. Examining the frequency of the nearly-sinusoidal curve shows that the frequency scales with the square root of the current as shown in Fig. 3 as one would expect for the ROF of a semiconductor laser and we interpret it as such. That the first instability occurs at the ROF is in line with studies of conventional semiconductor lasers [25, 26]; the difference being that chaos quickly ensues with conventional devices. We therefore interpret the TEP pulse train as a mode-locked train, resulting from a resonance between the ROF and the external cavity frequency.

We stress that the evolution does not end at 1:11. However, as the ROF is slowly varying for higher currents, we find situations where the locking jumps stochastically between different ratios as the repetition rate is close to several different ROF subharmonics. The TEP pulses become ever sharper with increasing current as the number of harmonics grows. The appearance of these regular pulse trains signifies a phase-locking of ECMs with a high level of organization resulting from the resonance. The large number of higher order harmonics in the RF spectra with narrow widths at the detection resolution limit ( $\sim 1$  MHz) strongly supports our interpretation of the phenomenon as a new mode-locking mechanism. These narrow RF lines also confirm that the periodic traces observed are indeed stable. We also tested external cavity round-trip lengths of 0.5 m and 1.4 m and found the same qualitative behaviour. Thus, the mode-locking appears to be robust to control parameter variations. We note that the feedback does not result in any excitation of the other short-cavity modes, suppressed by the DFB grating. We also note that modal groupings leading to pulses with trailing edge plateaux seem to be

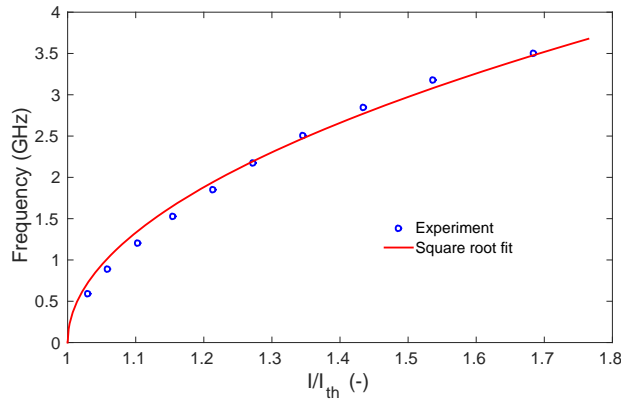


Fig. 3. Experimentally obtained frequencies of the nearly sinusoidal oscillations (black circles) as the injection current was varied. The red solid line shows a square root fit.

a common feature of mode-locked QD lasers: they have also been observed in [23] and more recently in [27]. In all cases, there is a dominant mode responsible for the plateaux observed.

### 3. Numerical model

We model the system as a laser consisting of two sections: namely, the semiconductor laser itself and the external cavity. The first section, of length  $L_{\text{int}}$ , is very short and contains the gain medium and the second section, of length  $L_{\text{ext}} \gg L_{\text{int}}$ , is empty. The equation describing the evolution of the electric field envelope  $E(t)$  is

$$\gamma^{-1} \frac{dE}{dt} + E(t) = \sqrt{\kappa} \exp((1 - i\alpha)G(t - \tau)/2 + i\phi) E(t - \tau) + \varepsilon \exp((1 - i\alpha)G(t - \tau - T)/2 + i\psi) E(t - \tau - T) \quad (1)$$

and is a generalization of the field equation in [28, 29].  $E(t)$  is the normalized complex amplitude of the electric field, while  $t$  is the time normalized by the short cavity round-trip time. The dimensionless time delays  $\tau$  and  $T$  correspond to the short and long cavity round-trip times, determined by the cavity lengths  $L_{\text{int}}$  and  $L_{\text{ext}}$ , respectively. The attenuation factor  $\kappa < 1$  describes total non-resonant linear intensity losses per cavity round-trip,  $\gamma$  is the dimensionless bandwidth of the cavity, and  $\alpha$  is the linewidth enhancement factor. We note that regardless of the feedback level no other modes of the short 900  $\mu\text{m}$  cavity were excited experimentally allowing us to limit the value of the bandwidth in the model.  $\varepsilon$  describes the feedback strength and the phases  $\phi$  and  $\psi$  are control parameters determined by the detuning of the frequency of the gain maximum from the optical frequency of the closest cavity mode. Although the phase amplitude coupling in QD lasers can be a complicated variable, [30], we here assume a constant  $\alpha$  for mathematical simplicity while maintaining the essential physics of the system.

An appropriate set of QD carrier equations are also required. The variable  $G(t)$  is the normalized gain defined by

$$G(t) \equiv 2gL_{\text{int}}[2\rho_g(t) - 1], \quad (2)$$

where  $\rho_g(t)$  describes the ground state (GS) dot occupation probability and  $g$  is the effective gain factor. The evolution of the occupation probabilities satisfy the following equations

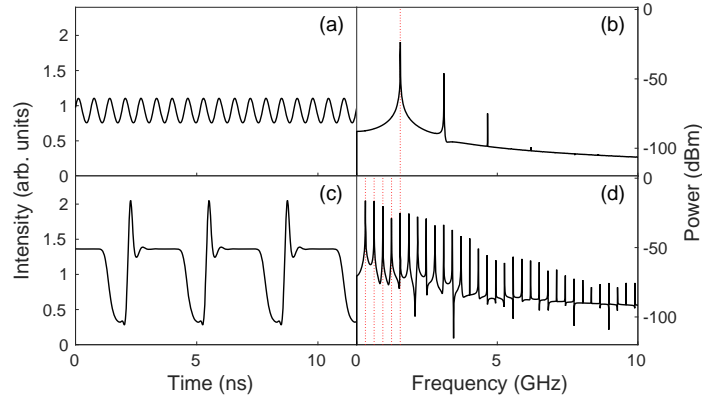


Fig. 4. Numerical traces showing (a) the nearly sinusoidal RO time series, (c) the fundamental TEP pulse train and (b) and (d) the corresponding RF spectra, respectively. The parameters are  $\varepsilon = 0.1375$  (a) and  $\varepsilon = 0.2$  (b);  $N_0 = 10$ ,  $\kappa = 0.3$ ,  $\phi = 2$  and  $\psi = 4$ . The two frequencies are in a ratio of 1:5 in this case.

$$\eta^{-1} \frac{d\rho_g}{dt} = -\rho_g + 2F(\rho_g, \rho_e) - (e^G - 1) |E|^2, \quad (3)$$

$$\eta^{-1} \frac{d\rho_e}{dt} = -\rho_e - F(\rho_g, \rho_e) + D(\rho_e, N), \quad (4)$$

$$\eta^{-1} \frac{dN}{dt} = N_0 - N - 4D(\rho_e, N), \quad (5)$$

where  $\rho_e(t)$  describes the excited state (ES) dot occupation probability and  $N(t)$  the carrier density in the wetting layer, scaled to the QD carrier density.  $\eta \equiv \tau\tau_c^{-1} \ll 1$  where  $\tau_c$  denotes carrier recombination time. The dimensionless parameter  $N_0$  describes the pumping process in the gain section. The factors 2 and 4 in Eqs. (2) and (5) account for the spin degeneracy in the QD energy levels. The function  $D(\rho_e, N)$  describes the carrier exchange rate between the wetting layer and the ES of the dots. In its most general form, this carrier exchange is formulated as

$$D(\rho_e, N) = R_w^{cap} (1 - \rho_e) - R_w^{esc} \rho_e, \quad (6)$$

where  $R_w^{cap} \equiv BN$  describes the carrier capture from the wetting layer to the dots with rate  $B$ .  $R_w^{esc}$  a temperature-dependent coefficient corresponding to carrier escape from the dots to the wetting layer.  $F(\rho_g, \rho_e)$  describes carrier exchange between the GS and ES of the dots and can be written as:

$$F(\rho_g, \rho_e) = R^{cap} (1 - \rho_g) - R^{esc} (1 - \rho_e), \quad (7)$$

where  $R^{cap} \equiv B\rho_e$  and  $R^{esc} \equiv C\rho_g$  define the energy exchange between the GS and ES. The  $(1 - \rho_{e,g})$  factors describe Pauli blocking in the expressions (6) and (7). Equations (1)-(5) are in dimensionless form. For the numerical simulations we choose common material parameters for QD lasers. We consider  $\eta = 0.1$  ( $\eta = \tau\tau_c^{-1}$  where  $\tau = 100$  ps is the short cavity round-trip time and  $\tau_c \sim 1000$  ps is the recombination time),  $\alpha = 4$ ,  $B = 100$ ,  $C = 10$ ,  $R_w^{esc} = 1$ ,  $2gL_{int} = 4$  and

the rescaled dimensionless time delays are  $\tau = 1$  and  $\tau + T = 31 \gg \tau$ . The narrow bandwidth  $\gamma = 1.2$  of the cavity was chosen to match the single mode operation provided by the DFB. The numerical parameters were chosen in order to match the two most important laser time scales: the ROF and external cavity round-trip time.

Direct simulations reproduce the experimental findings extremely well. For low feedback strengths, the output has a constant intensity. Increasing the feedback strength, a periodic, almost sinusoidal trace is eventually obtained as seen in Fig. 4(a). The frequency of this trace is the ROF. Increasing the feedback strength still further yields a TEP pulse train. As with the experiment, the ratio between the ROF and the external cavity frequency can be varied depending on the cavity length and injected current. Figure 4 shows the case for a 1:5 ratio and the correspondence with the experiment is excellent. It is worth noting here that the amplitude of the oscillations in the sinusoidal trace at the ROF is significantly smaller than that of the TEP pulse train, as also observed in the experiment.

As the feedback strength is further increased, more complex patterns were obtained. These include the evolution from single to multipulse trains similar to those observed in the experiment. Numerically we find that the system is highly multistable with different pulse trains possible for the same control parameters. We note that variations of the phases  $\phi$  and  $\psi$  may sufficiently affect the pulse shapes and the locking ranges as could be expected, but do not change the scenario of the resonant mode locking qualitatively.

This evolution of dynamics is in stark contrast to that observed with conventional semiconductor lasers. The key property of QD lasers in this phenomenon is the high damping of the ROs. With conventional semiconductor lasers the ROs become undamped at very low feedback strengths and chaos quickly follows. The high damping in QD lasers allows the lasers to remain stable up to the high feedback levels required for the mode-locking mechanism to take effect.

The physics of the phenomenon can be understood as follows: At the onset of the first instability a Hopf bifurcation occurs corresponding to an undamping of the ROs. This yields coherent sidebands around the central optical frequency. When these are close to external cavity mode frequencies they can in turn excite these via optical injection yielding new modes coherent with the central tone. A second Hopf bifurcation then arises at the round-trip frequency and the sidebands that result here can inject and excite neighbouring external cavity modes.

#### 4. Conclusion

In conclusion, we have uncovered a new mode-locking mechanism in semiconductor lasers. The ECMs in QD lasers undergoing moderately high levels of external optical feedback become mutually phase-locked via a resonance with the ROF. The resonance takes the form of rational ratios between the external cavity repetition rate and the ROF. Depending on the control parameters of the system, different ratios of the frequencies are possible. The mechanism relies on the high RO damping in these devices which allows high feedback strengths to be tolerated without the generation of chaos.

#### Acknowledgments

This work was conducted under the framework of the INSPIRE programme funded by the Irish Government's Programme for Research in Third Level Institutions Cycle 5, National Development Plan 2007-2013 with the assistance of the European Regional Development Fund. The authors also gratefully acknowledge the support of Science Foundation Ireland under Contracts No. 11/PI/1152 and 12/RC/2276. The authors in Brussels acknowledge support of the Fonds National de la Recherche Scientifique (Belgium).